ARTICLE
Integrative Medicine Discovery 2025;9:e25016. https://doi.org/10.53388/IMD202509016

UPLC/MS-MS-based pharmacokinetics of phytosterol magnetic targeted drug delivery system in rat and tissue distribution in mouse

Xiao-Yu Wang[1], Wen-Jing Chen[1], Yi-Fan Mao[1], Jun-Li Zhang[1], Hai-Ting Zhu[1], Hui-Nan Wang[1], Ming-Rui Jiang[1], Xin-Ning Zhang[1], Peng Xu[1], Ying-Zi Wang[1*]

[1]School of Chinese Materia Medica, Beijing University of Chinese Medicine, Beijing 102488, China.

[*]**Correspondence to:** Ying-Zi Wang, School of Chinese Materia Medica, Beijing University of Chinese Medicine, Sunshine South Street, Fangshan District, Beijing 102488, China. E-mail: wangyzi@sina.com.

Author contributions

Wang XY was responsible for the conception and design of the study, data analysis and interpretation, and manuscript writing, and approved the final manuscript. Wang YZ provided administrative support and approved the final manuscript. Chen WJ and Mao YF contributed to the collection of data and approved the final manuscript. Zhu HT, Zhang JL, Zhang XN, Jiang MR, Wang HN, and Xu P contributed to data analysis and interpretation and approved the final manuscript. All authors read and approved the final manuscript.

Competing interests

The authors declare no conflicts of interest.

Acknowledgments

This work was sponsored by the Fundamental Research Funds forthe Central Universities (No. 2024-JYB-JBZD-047); High Level Key Discipline Construction of Traditional Chinese Medicine (zyyzdxk-2023272).

Abbreviations

AUC, area under the curve; C_{max}, maximum concentration; EFL_1, Euphorbia factors L_1; RSD, relative standard deviation; MRT, mean residence time; UPLC-MS/MS, ultra-performance liquid chromatography-tandem massspectrometry.

Citation

Wang XY, Chen WJ, Mao YF, et al. UPLC/MS-MS-based pharmacokinetics of phytosterol magnetic targeted drug delivery system in rat and tissue distribution in mouse. *Integr Med Discov*. 2025;9:e25016. doi: 10.53388/IMD202509016.

Peer review information

Integrative Medicine Discovery thanks Zhi-Dong Liu and Yi Ding for their contribution to the peer review of this paper.

Executive editor: Meng-Meng Song.

Received: 22 January 2025; **Revised:** 22 April 2025; **Accepted:** 11 June 2025; **Available online:** 12 June 2025.

Abstract

Background: Building upon our previous work that developed a folate receptor-mediated, euphaorbia factor L1-loaded PLGA microsphere system integrating active and magnetic targeting for theranostics, further investigation into its in vivo pharmacokinetics and tissue distribution is warranted despite its demonstrated biocompatibility and safety. **Methods:** A UPLC-MS/MS method was established to determine the concentration of euphorbia sterol in rat plasma and mouse tissue homogenates, healthy male SD rats and KM mice were administered in groups, drug concentrations at different time points were determined, pharmacokinetic parameters were analyzed by DAS software, and data were processed by SAS software. **Results:** The proposed method met the requirements of biological sample detection. The plasma pharmacokinetics of rats showed that the drug concentration in the microsphere group was lower than that in the injection group, and the parameters such as mean residence time ($MRT_{(0-t)}$), half-life ($T_{1/2z}$) and apparent volume of distribution (V_z) were significantly different from those in the solution group. The distribution of mouse tissues showed that the drug concentrations in the liver and lung tissues of the microsphere preparation group were higher than those in the injection group, and the drug concentrations in the lung and liver tissues were more distributed. **Conclusion:** The targeted drug delivery system changed the pharmacokinetic behavior and tissue distribution of euphorbia sterol, slowed down plasma elimination, prolonged the half-life, and improved the targeting of drugs in lung and liver tissues and the magnetic targeting effect of lungs.

Keywords: euphorbia sterol; magnetic targeted drug delivery system; pharmacokinetics; tissue distribution

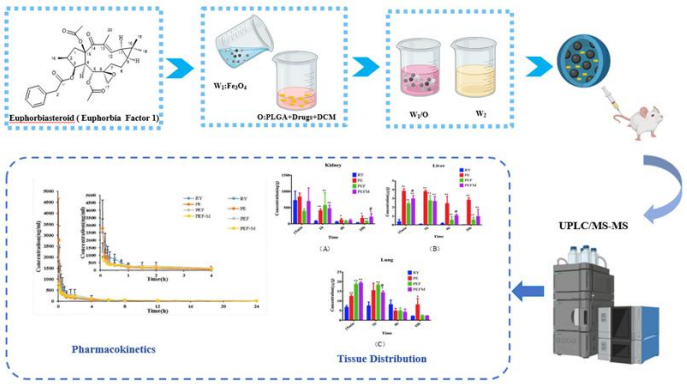

Introduction

Euphorbia sterol is a diterpenoid ester compound extracted from the dried mature seeds of *Euphorbia lathyris* L., which has strong anti-tumor activity and reversal of tumor multidrug resistance [1–5]. However, due to their poor water solubility and low oral bioavailability, the further clinical development and application of euphorbia lathyris dieneol have been limited. Previously, our research group, based on the theory of folate receptor-ligand mediated targeted therapy and the integrated research idea of diagnosis and treatment, coloaded the lipid-soluble drug euphorbia lathyris dieneol and the water-soluble nanomaterials into the degradable carrier PLGA to prepare folate-targeted PLGA microspheres containing euphorbia lathyris dieneol, constructing a dual-targeting drug delivery system of active targeting and magnetic targeting. This system has the advantages of biodegradability, high clinical safety, stable drug loading and encapsulation efficiency, as well as good biocompatibility and safety. However, the pharmacokinetics and tissue distribution of euphorbia lathyris dieneol in the organism are still unclear. Therefore, in order to evaluate the targeted therapeutic effect of this drug delivery system, based on the previous research and literature review, this study uses ultra-performance liquid chromatography-tandem massspectrometry (UPLC-MS/MS) to establish a method for determining the drug concentration in rat plasma biological samples and mouse tissue homogenates of the magnetic targeted drug delivery system of euphorbia lathyris dieneol, compares the pharmacokinetic characteristics of the magnetic targeted preparation of euphorbia lathyris dieneol in healthy rats, and elaborates on the pharmacokinetic changes and differences of euphorbia lathyris dieneol caused by the microsphere preparation from the perspective of pharmacy. It also investigates and compares the influence of the construction of the microsphere drug delivery system on the tissue and organ distribution characteristics of euphorbia lathyris dieneol in KM mice and the distribution differences. The aim is to provide a reference for improving the targeted therapeutic effect of euphorbia lathyris dieneol on tumors.

Materials

Materials and reagents

Abispoyleol (Abispoylein L1 reference substance, batch 111789-200901; National Institutes for Food and Drug Control, Beijing, China; purity 99.3%), wogonin (internal standard, batch YS0925SA13; Shanghai Yuanye Bio-Technology Co., Ltd., Shanghai, China; purity ≥ 98%), methanol (MS-grade; Thermo Fisher Scientific, Waltham, MA, USA), formic acid (HPLC-grade; Dikma Technologies Inc., Beijing, China), dimethyl sulfoxide (DMSO; Sigma-Aldrich, St. Louis, MO, USA), ethyl acetate (analytical grade; Beijing Chemical Works, Beijing, China), sodium chloride injection (normal saline, medicinal grade; Shijiazhuang No. 4 Pharmaceutical Co., Ltd., Shijiazhuang, China), polyoxyethylene castor oil (Cremophor® EL; Sigma-Aldrich, Steinheim, Germany), ACQUITY UPLC® BEH C18 Column (1.7 μm, 2.1 × 50 mm; Waters Corporation, Milford, MA, USA; P/N 186002350).

Instrument

Ultra-high performance liquid chromatography-tandem quadrupole mass spectrometer (Acquity UPLC-Xevo TQ-S; Waters Corporation, Milford, MA, USA), high-speed electric homogenizer (T10 basic; IKA Werke GmbH & Co. KG, Staufen, Germany), high-speed refrigerated centrifuge (Eppendorf 5810 R; Eppendorf AG, Hamburg, Germany), DCY series nitrogen evaporator (Qingdao Haike Instrument Co., Ltd., Qingdao, China), vortex mixer (MX-S/F; Dalong Xingchuang Laboratory Instrument Co., Ltd., Beijing, China), multi-position magnetic stirrer (HJ-6A; Changzhou Guohua Electric Appliance Co., Ltd., Changzhou, China), analytical balance (BSI10S; Sartorius AG, Göttingen, Germany), ultrasonic cleaner (KH-7200DB; Kunshan Ultrasonic Instruments Co., Ltd., Kunshan, China), Milli-Q water purification system (Merck Millipore, Burlington, MA, USA).

Experimental animals

Healthy male Sprague-Dawley (SD) rats (10-week-old, SPF grade, ~ 200 g) were purchased from Sibelfu Experimental Animal Technology Co., Ltd. (Certificate No. 11401500016708) and housed in SPF-grade facilities at the university experimental animal center with free access to food and water and adaptive feeding.

Healthy male Kunming (KM) mice (3-week-old, SPF grade, ~ 20 g) were obtained from Subei Experimental Animal Technology Co., Ltd. (License No. SCXK (Jing) 2016-0002) and maintained under identical SPF conditions with ad libitum feeding.

All procedures were approved by the Institutional Animal Care and Use Committee (IACUC Approval No. BUCM-4-2021092205-3093) and strictly adhered to the Guide for the Care and Use of Laboratory Animals (NIH Publication No. 8023, 8th Edition, 2011).

Experimental method

UPLC-MS/MS chromatographic conditions

For rat plasma biological samples, an ACQUITY UPLC® BEH C18 column (50 mm × 2.1 mm, 1.7 μm) was used. The mobile phase was methanol (A)–0.1% formic acid (B), and the gradient elution program was as follows: 0–0.5 min, 30% A; 0.5–1.5 min, 30%–80% A; 1.5–3.0 min, 80% A; 3.0–5.0 min, 30% A. The flow rate was 0.4 mL/min, the detection wavelength was 275 nm, the detection column temperature was 30 ˚C, and the injection chamber temperature was 4 ˚C. For mouse tissue homogenate, an ACQUITY UPLC® BEH C18 column (50 mm × 2.1 mm, 1.7 μm) was used. The mobile phase was methanol (A)–0.1% formic acid (B), and the gradient elution program was as follows: 0–0.5 min, 30% A; 0.5–2.5 min, 30%–60% A; 2.5–4.5 min, 60%–75% A; 4.5–5.5 min, 75%–95% A; 5.5–7.0 min, 95% A; 7.0–8.0 min, 95%–30% A; 8.0–10.0 min, 30% A. The flow rate was 0.4 mL/min, the detection wavelength was 275 nm, the detection column temperature was 30 ˚C, and the injection chamber temperature was 4 ˚C.

UPLC-MS/MS mass spectrometry conditions

The electrospray ionization source (ESI) was used, with the ionization mode being positive ion mode and the scanning mode being multiple reaction monitoring (MRM). The capillary voltage was 3.0 kV, and the desolvation gas temperature. At 400 ˚C, the desolvation airflow rate is 800 L/h, and the cone airflow rate is 150 L/h.

Method for handling biological samples

A total of 100 μL of rat plasma sample and mouse tissue homogenate were placed in a 2 mL EP tube with stopper, and 20 μL of 50 μg/L and 500 μg/L wogonin internal standard solution were added respectively. After vortex mixing for 1 min, 1 mL of ethyl acetate was added for vortex for 5 min, and centrifuged at 7,000 g for 15 min and 10 min, respectively. Then 800 μL of upper ethyl acetate was taken, and 1 mL of ethyl acetate was added for vortex for 5 min, centrifuged at 7,000 g for 15 min, and 900 μL of upper ethyl acetate was taken, and the two extracts were combined [6–9]. The ventilation cupboard was blown dry with nitrogen at 37 ˚C and stored at −20 ˚C. Before injection analysis, the residue was redissolved with 100 μL mobile phase (methanol), vortexed for 1 min, centrifuged at 7,000 g for 10 min, and the supernatant was detected and analyzed by UPLC-MS/MS.

Methodological investigation

Methodological validation was carried out according to the guidelines of the US Food and Drug Administration (FDA).

Specifically. Precisely aspirate 100 μL of rat plasma samples and blank tissue homogenates of mice. Operate and conduct the analysis in accordance with the method under “Method for handling biological samples” to obtain the ion current chromatograms of each group of samples.

Examination of linear relationship. The reference solution of quinolide sterol was respectively taken to prepare a series of standard

solutions, and then diluted with blank plasma or blank tissue homogenate to form analytical sample solutions of corresponding concentrations. The linear equation and correlation coefficient were calculated using UPLC-MS/MS software.

Precision and repeatability. Low, medium and high concentrations of quality control (QC) samples were respectively prepared from blank biological samples. The intra-day precision and inter-day precision of QC samples,as well as the repeatability under different concentrations were calculated.

Stability. Different concentrations of milfoil sterol sample solutions were prepared respectively using blank plasma or blank tissue samples. They were treated as described in "Method for handling biological samples" to investigate their stability after three freeze-thaw cycles and 4 h at room temperature.

Matrix effect and recovery rate. The blank samples (blank plasma for rats and blank tissue homogenate for mice) were extracted with ethyl acetate according to the "Method for handling biological samples", and the same concentration of internal standard and low, medium, and high series standard solutions were added respectively. After drying with a nitrogen blow dryer, the solutions were reconstituted with 100 μL mobile phase by vortex mixing, centrifuged at 8,000 r/min for 10 min, and the supernatant was injected to obtain the concentration C1. The blank samples (plasma for rats and tissue homogenate for mice) were treated with low, medium, and high series standard solutions and the corresponding concentration internal standard solution according to their respective sample treatment methods to obtain the concentration C2. Additionally, the mobile phase was used to prepare the abovementioned low, medium, and high standard solutions and internal standard solutions of the corresponding concentrations to obtain the concentration C3. Among them, C1/C3 is the matrix effect, and C2/C1 is the recovery rate.

Animal administration regimens and sample collection

Pharmacokinetic study in rats. Healthy SD rats, male, were randomly divided into the EFL_1 (RY) solution group, the PLGA-EFL_1 (PE) group, the PLGA-EFL_1-Fe_3O_4 (PEF) group, and the PLGA-EFL_1-Fe_3O_4 (PEFM) plus magnetic group. Before the experiment, the rats were fasted for more than 12 h without water. The next day, the rats were given the above preparations at a dose of 10 mg/kg (based on the stigmasterol content) through the tail vein in the early morning. Blood samples were collected from the ocular fundus venous plexus of the rats at 0 h before administration and at 0.08 h (5 min), 0.17 h (10 min), 0.25 h (15 min), 0.33 h (20 min), 0.5 h (30 min), 0.75 h (45 min), 1, 1.5, 2, 4, 6, 8, 12, and 24 h after administration, and placed in anticoagulated tubes with sodium heparin. The samples were centrifuged at 7,000 g for 10 min, and the supernatants were separated and stored at −20 °C for future testing. After 4 h of the experiment, the normal diet of the animals was restored.

Research on tissue distribution in mice. Healthy male KM mice; before the experimental administration, the mice were fasted for 12 h and had free access to drinking water. They were randomly divided into 4 groups: EFL_1 (RY) group, PLGA-EFL_1 (PE) group, PLGA-EFL_1-Fe_3O_4 (PEF) group, PLGA-EFL_1-Fe_3O_4 (PEFM) plus magnetic group. The above preparation was given through the tail vein at a dose of 14 mg/kg (based on milneantriol),and the animals were sacrificed at four time points of 15 min, 1 h, 4 h and 10 h after administration. The tissues such as the liver, lungs and kidneys were promptly removed. The bloodstains and contents on the surface of the tissues were washed away with normal saline and dried with filter paper. They were weighed and set aside for homogenization before determination.

Statistical analysis

The experimental data were processed by SAS 9.3 statistical software (SAS Institute Inc., Cary, NC, USA), expressed as $x \pm s$, t test was used to compare the two groups, $P < 0.05$ was considered as significant difference, $P < 0.01$ was considered as very significant difference. The pharmacokinetic parameters were calculated by DAS 2.0 (Mathematical Pharmacology Professional Committee, Chinese Pharmacological Society, Beijing, China) and the drug-time curve was drawn.

Result

Methodological testing results

Specificity. The ion current chromatograms of rat plasma and mouse tissue samples obtained by the specificity test are shown in Figure 1 and Figure 2, indicating that the endogenous substances in the tissues do not interfere with the determination of abenzoate and the internal standard wogonin. The established method has good specificity.

Examination of linear relationship. The linearity of quinolide sterol in rat plasma within the range of 5–500 ng/mL was good, with the linear equation being Y = 0.0710609X + 0.119467, r = 0.9993; The linear equations, correlation coefficients, and linear ranges of quinolide sterol in different tissues of mice are shown in Table 1. The examination results of the linear relationship indicate that quinolide sterol under each matrix shows a good linear relationship within the linear concentration range.

Precision and repeatability. It can be known from Table 2 and Table 3 that the relative standard deviation (RSD) of the intra-day and inter-day precision of quinolizidine in rat plasma and different tissue samples of mice is less than 15.0%, while the corresponding accuracy is within 5%. These data indicate that this method is reliable, with good reproducibility and accuracy, and complies with the requirements for quantitative determination of biological samples.

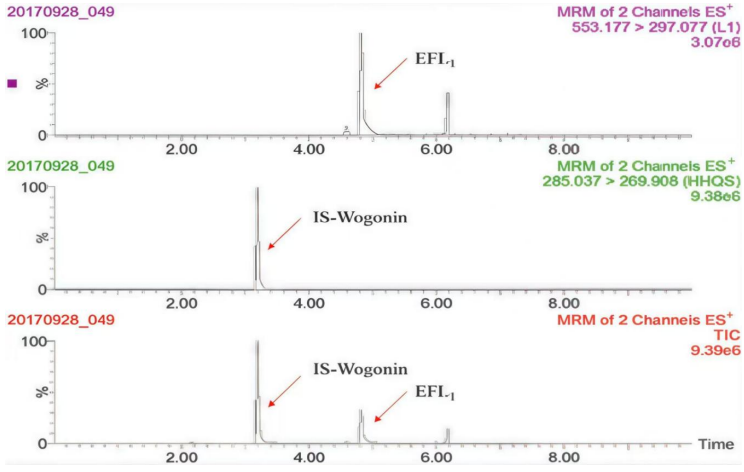

Figure 1 Total ion chromatorgraphy of EFL_1 in rat plasma.

MRM, Multiple Reaction Monitoring; ES^+, Electrospray Ionization; HHQS, High High Quadrupole Setting; TIC, Total Ion Chromatogram; IS Wogonin, Internal Standard Wogonin.

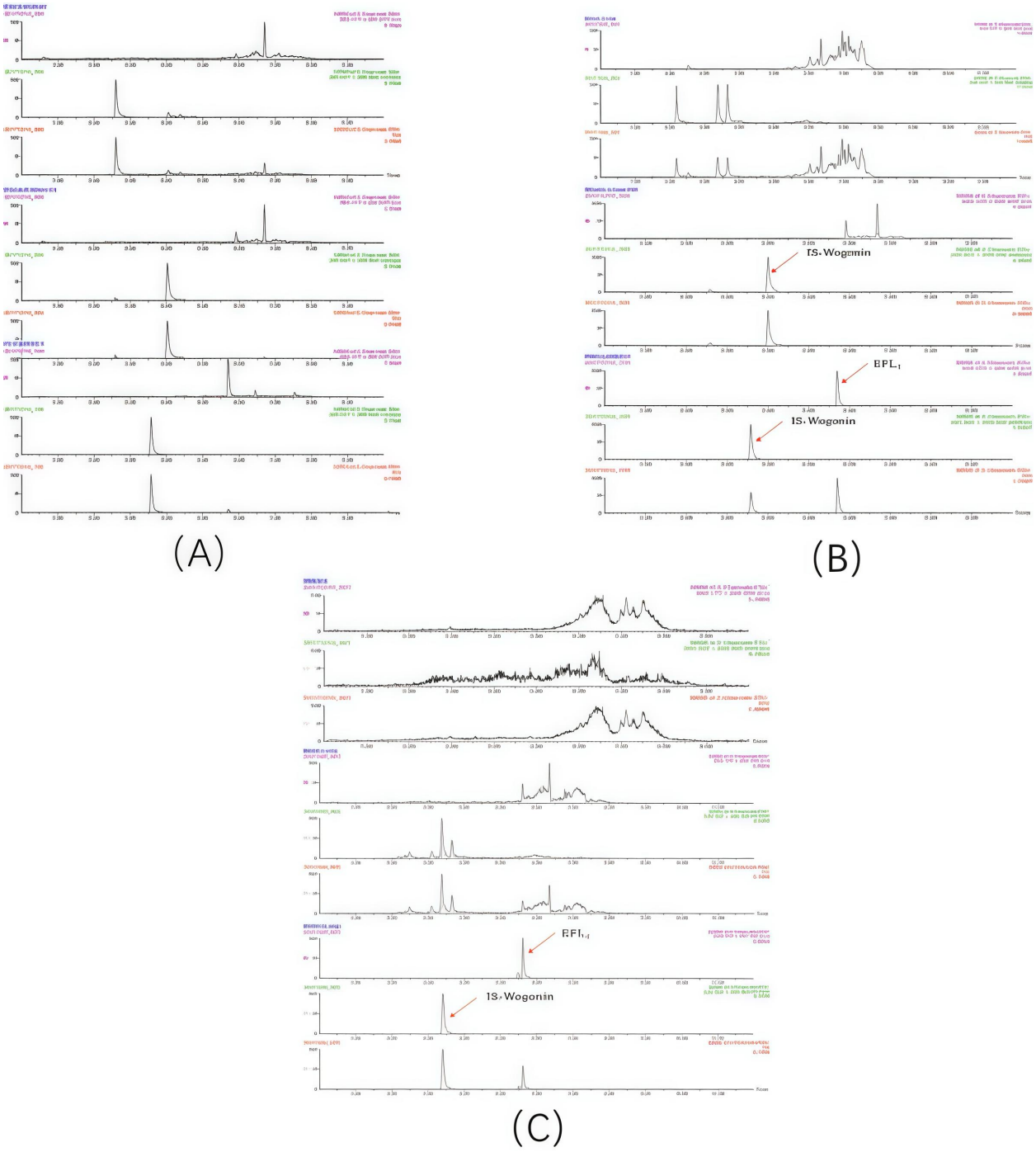

Figure 2 Total ion current plots of EFL_1 in tissue.
(A) kidney tissue; (B) liver tissue; (C) lung tissue. MRM, Multiple Reaction Monitoring; ES^+, Electrospray Ionization; HHQS, High High Quadrupole Setting; TIC, Total Ion Chromatogram; IS Wogonin, Internal Standard Wogonin.

Table 1 Linear relationship of EFL_1 in mice tissues (n = 3)

Tissue	Regression equation	r	Linear range (ng/mL)
Kidney	Y = 0.03865X + 0.5005	0.9995	10–1,500
Liver	Y = 0.03134X + 0.2087	0.9994	10–1,500
Lung	Y = 0.03389X + 0.0764	0.9998	10–2,000

Table 2 Precision of EFL_1 in rat plasma (n = 3)

Concentration (ng/mL)	RSD (%)	
	Intra-day precision	Inter-day precisions
20	6.76	6.76
200	6.62	8.22
500	5.10	5.10

RSD, relative standard deviation.

Table 3 Precision of EFL_1 in different tissues of mice (n = 3)

Tissue	Concentration (ng/mL)	RSD (%)	
		Intra-day precision	Inter-day precisions
Kidney	20	12.13	9.45
	500	3.01	5.25
	1,000	4.68	5.98
Liver	20	6.00	8.14
	500	2.00	3.50
	1,000	4.74	5.02
Lung	20	2.98	5.69
	500	2.91	3.41
	1,000	3.16	2.31

RSD, relative standard deviation.

Stability. The stability of rat plasma and different tissues of mice is shown in Table 4 and Table 5. After three freeze-thaw cycles and being placed at room temperature for 4 h, the RSD at each concentration was less than 15%, indicating that the stability of rat plasma and mouse tissues was good, which met the requirements for the determination and analysis of biological samples.

Matrix effect and extraction recovery. The matrix effect and extraction recovery of euphorbia sterol in rat plasma and mouse tissues are shown in Table 6 and Table 7. The recovery rate of euphorbia sterol was between 83.86–109.33%. At the same time, the range of matrix effect was 86.88–114.32%. The results showed that the recovery rate of the method was good, and the matrix material did not interfere with the detection of compounds.

Pharmacokinetic results in rats

After intravenous injection of PLGA-EFL_1 and other preparations in rats, the data of the changes in blood drug concentration over time were plotted into the drug-time curve, as shown in Figure 3. The main pharmacokinetic parameters are presented in Table 8. The in vivo pharmacokinetic characteristics of the microsphere preparation group and the Thunbaja sterol solution group are significantly different. The initial concentration of EFL_1 in the solution group is relatively high, while the blood drug concentration time curves of the PE and PEF preparation groups are relatively gentle and prolonged, and the retention time of the drug in the body is longer. Compared with the RY solution group, PLGA-EFL_1 (PE) and PLGA-EFL_1-Fe_3O_4 (PEF), the pharmacokinetic process in the rats of the preparation group has undergone certain changes. The initial drug concentration C0 after administration was lower than that of the solution group, suggesting a lower drug concentration in the blood. The apparent volume of distribution (Vz) increased from 0.03 L/kg to 0.078 L/kg, 0.109 L/kg, and 0.067 L/kg respectively, which were 2.6, 3.63, and 2.23 times that of the solution group, suggesting that the microspheres and magnetic microsphere preparations may be more distributed to various tissues and organs after entering the body. The mean residence time (MRT) was 1.43, 1.46, and 1.20 times that of the solution group respectively, and the elimination half-life ($T_{1/2z}$) was 2.54, 2.34, and 1.72 times respectively, indicating that both PLGA-EFL_1 and PLGA-EFL_1-Fe_3O_4 (the nonmagnetic field PEF group and the magnetic field PEFM group) have a certain sustained-release effect,with slow elimination in vivo. At the same time, the elimination of the group with magnetic materials added was slower than that of the PLGA-EFL_1 group, while the elimination was slightly faster after adding a magnetic field with a certain magnetic field strength than without adding a magnetic field.

Tissue distribution results in mice

The concentration of quinolide in various tissues of mice is shown in Figure 4. Through experiments, it can be known that the distribution pattern of drug concentration in mouse tissues and organs is lung > liver > kidney. After quinolide was prepared into microsphere preparations, the drug concentration in the lung tissue was significantly increased. At the same time, the addition of the magnetic field had an impact on the distribution of quinolide drug concentration in the magnetic microsphere preparations, preliminarily proving the pulmonary magnetic targeting effect of the quinolide magnetic targeted drug delivery system in healthy animals.

Discussion

Euphorbia sterol has strong anti-tumor activity and reversal of tumor multidrug resistance. However, due to its poor water solubility and low oral bioavailability, its further clinical development and application are limited. In the previous study, our group constructed a magnetic targeting drug delivery system with active targeting and magnetic targeting. At the same time, the in vitro release behavior of the magnetic targeting microspheres under different pH conditions was investigated by constant temperature water bath oscillation method, and a method for the determination of euphorbia sterol in biological samples of intestinal perfusate was established .On this basis, this study used UPLC-MS/MS to establish a method for the determination of drug concentration in rat plasma biological samples and mouse tissue homogenates in the magnetic targeted drug delivery

Table 4 Stability of EFL_1 at different storage conditions in rat plasma (n = 3)

Concentration (ng/mL)	RSD (%)	
	Three freeze-thaw cycles	Stability at room temperature
20	12.73	7.2
200	10.61	3.63
500	10.09	2.52

RSD, relative standard deviation.

Table 5 Stability of EFL_1 in different tissues of mice (n = 3)

Tissue	Concentration (ng/mL)	RSD (%)	
		Three freeze-thaw cycles	Stability at room temperature
Kidney	20	4.86	7.75
	500	11.03	11.11
	1,000	1.42	3.98
Liver	20	6.48	3.57
	500	1.19	0.75
	1,000	3.97	5.62
Lung	20	10.91	7.82
	500	1.90	0.86
	1,000	6.98	2.71

RSD, relative standard deviation.

Table 6 Recovery rate and matrix effect of EFL_1 in rat plasma (n = 3)

Concentration (ng/mL)	Mean (%)		RSD (%)	
	Recovery rate	Matrix effect	Recovery rate	Matrix effect
20	90.7	95.38	2.07	7.72
200	100.47	97.88	6.13	2.81
500	102.14	99.05	2.18	4.62

RSD, relative standard deviation.

Table 7 Recovery rate and matrix effect of EFL_1 in different tissues of mice (n = 3)

Tissue	Concentration	Mean (%)		RSD (%)	
		Recovery rate	Matrix effect	Recovery rate	Matrix effect
Kidney	20	92.08	100.16	7.95	7.28
	500	92.02	104.44	8.55	8.70
	100	90.88	94.98	5.19	2.44
Liver	20	101.42	96.84	7.13	6.61
	500	97.36	101.06	2.18	1.04
	1,000	92.49	97.29	6.45	4.16
Lung	20	97.02	96.30	1.63	0.85
	500	100.39	101.62	5.49	3.86
	1,000	90.60	95.24	5.96	3.59

RSD, relative standard deviation.

Table 8 The mean non-compartmental plasma pharmacokinetic parameters of EFL_1 after intravenous admistration to SD rats in rat plasma

Data	Unit	RY solution	PE NP	PEF NP	PEFM NP
$T_{1/2z}$	h	4.92 ± 0.88	12.49 ± 9.07*	11.51 ± 5.50*	8.47 ± 1.64
C_{max}	mg/L	2,980.96 ± 854.86	2,093.16 ± 1,056.28	1,053.26 ± 167.06	823.84 ± 94.93
$AUC_{(0-t)}$	mg/L × h	2,316.57 ± 613.67	1,865.02 ± 1,078.99	1,203.99 ± 312.17	1,559.21 ± 304.89
$AUC_{(0-\infty)}$	mg/L × h	2,349.57 ± 646.20	2,320.28 ± 1,494.72	1,466.83 ± 587.87	1,675.18 ± 302.67
$MRT_{(0-t)}$	h	3.74 ± 0.78	5.34 ± 0.87*	5.45 ± 1.66*	4.50 ± 0.61*
$MRT_{(0-\infty)}$	h	4.12 ± 1.09	12.54 ± 9.74	11.75 ± 5.85	6.70 ± 0.32
V_z	L/kg	0.03 ± 0.01	0.08 ± 0.06*	0.11 ± 0.03**	0.07 ± 0.02
CL_z	L/h/kg	0.004 ± 0.002	0.004 ± 0.002	0.007 ± 0.002*	0.006 ± 0.001

The PLGA-EFL_1 (PE NP), PLGA-EFL_1-Fe_3O_4 (PEF NP) and PLGA-EFL_1-Fe_3O_4 with magnetic field (PEFM NP) preparation groups were compared with the solution group, respectively, $^{*}P < 0.05$, $^{**}P < 0.01$.

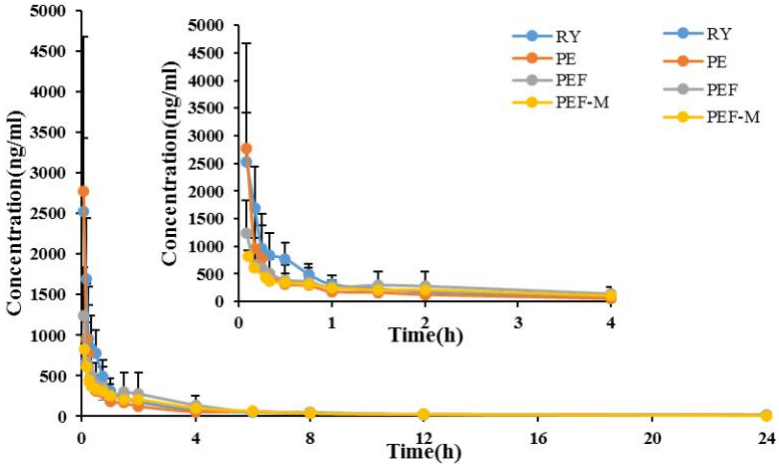

Figure 3 Blood level-time curve of RY solution, PLGA-EFL_1, PLGA-EFL_1-Fe_3O_4 and PLGA-EFL_1-Fe_3O_4 with magnetic field in rat plasma

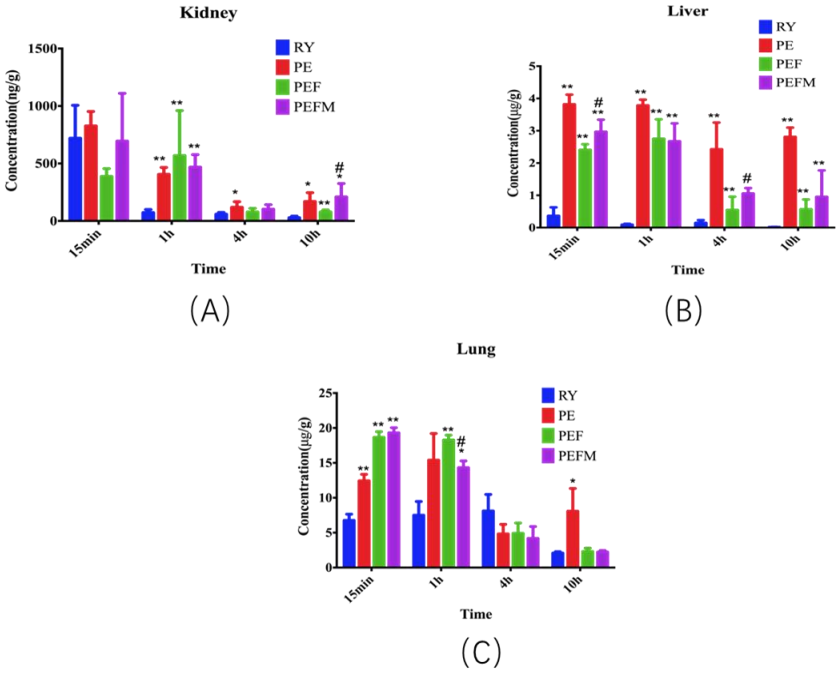

Figure 4 The concentration-time profile of EFL_1 in kidney, liver and lung tissue homogenates after i.v administration of EFL_1 (14 mg/kg) to mice.

$^{*}P < 0.05$ vs. control group; $^{**}P < 0.01$ vs. control group; $^{\#}P = 0.05$–0.10 (trend towards significance).

system of euphorbia sterol. Through methodological investigation, it was found that the impurity peaks in plasma and tissues did not interfere with the determination of analytical peaks, and the specificity, stability, precision and recovery rate all met the analysis requirements of biological samples.

The pharmacokinetic study showed that the plasma drug concentration of each microsphere group was lower than that of the injection group at the same dose, and the pharmacokinetic parameters such as $MRT_{(0-t)}$, $T_{1/2z}$ and apparent distribution volume (V_z) were significantly different from those of the solution group. The targeting and sustained-release effects of PLGA microspheres were preliminarily evaluated. However, the pharmacokinetic results showed that the microsphere preparation group did not effectively improve the bioavailability of euphorbia sterol in vivo. It has been reported that some fat-soluble drugs, such as docetaxel chitosan microspheres, have similar characteristics in pharmacokinetic studies [10–12]. It is speculated that microsphere preparations may make drugs more targeted to tissues and organs, thereby reducing drug utilization in plasma. On the other hand, some of the microspheres may be captured by the reticuloendothelial system (RES) and quickly remove the nanoparticles in the blood, failing to release the drug into the system circulation in time, resulting in no significant improvement in bioavailability [13–15]. At the same time, the complex physiological environment in vivo may further delay the degradation of PLGA skeleton, resulting in incomplete drug release [16–18]. In this study, the SD value of C_{max} plasma concentration in the solution group was larger (± 799 ng/mL) after tail vein administration, and there was a large individual difference in the absorption of drugs in rats. The pharmacokinetic characteristics in rats were consistent with established pharmacokinetic profiles reported in prior studies.

The results of tissue distribution experiment showed that the concentration of euphorbia sterol in lung, liver and kidney tissues of the three preparations showed a trend of lung > liver > kidney. In the kidney tissue, at 1 h and 10 h, there was a significant difference between the microsphere preparation group and the RY group, indicating that the microsphere preparation changed the distribution of euphorbia sterol in the kidney, and the drug concentration decreased slowly. It is speculated that the kidney has a slower clearance rate for the preparation group. In liver tissue, the concentrations of PE, PEF and PEFM preparation groups were significantly higher than those of RY solution group within 10 h, indicating that their liver targeting was significantly improved. In the PEF plus magnetic field group, the targeting was enhanced due to the magnetic field, which reduced the distribution of the drug in the non-target liver tissue. In lung tissue, the order of drug concentration at 15 min was PEF plus magnetic group > PEF group > PE group > RY group, and the difference between each preparation group and RY group was significant, indicating that the magnetic field at the initial stage of administration could make the drug rapidly target lung tissue. At 1 h, only PEF and PEFM groups were significantly different from RY group, and there was a significant difference in drug concentration between PEFM and PEF groups, indicating that the magnetic field changed the distribution of the carrier in the lung tissue. The drug concentration distribution of PEFM group in each tissue was compared with that of other preparation groups. Compared with the solution group, the drug concentration of PE, PEF and PEFM groups increased significantly at 15 min and 1 h, which may be due to the size effect of microsphere suspension, which made it easier to be taken up by developed organs of reticuloendothelial system, and the structure of pulmonary capillary network intercepted some microspheres . At the same time, the external magnetic field may be easier to capture nanoparticles from the pulmonary circulation system and increase the lung tissue retention rate of magnetically targeted nanoparticles [19, 20].

Conclusion

In summary, this study preliminarily explored the pharmacokinetics of euphorbia sterol magnetic targeted drug delivery system in vivo and its effect on the tissue distribution of euphorbia sterol in vivo. The results showed that the drug delivery system prolonged the half-life of euphorbia sterol in vivo, slowed down its plasma clearance rate, and improved the targeting of euphorbia sterol in liver and lung tissues. This study clarified the in vivo changes of the magnetic targeted drug delivery system of euphorbia sterol. Subsequently, the pharmacokinetic study of multi-dose administration will be carried out by expanding the sample, and the in vivo mechanism and metabolic mechanism of the drug will be revealed in depth, which will provide a basis for the determination of the dose and mode of administration in subsequent clinical studies.

References

1. Shi QW, Su XH, Kiyota H. Chemical and pharmacological research of the plants in genus Euphorbia. *Chem Rev*. 2008;108(10):4295–4327. Available at: http://doi.org/10.1021/cr078350s
2. Lee JW, Jin QH, Jang HR, et al. Lathyrane-Type Diterpenoids from the Seeds of Euphorbia lathyris L. with Inhibitory Effects on NO Production in RAW 264.7 Cells. *Chem Biodivers*. 2018;15(10):e1800144. Available at: http://doi.org/10.1002/cbdv.201800144
3. Chen XY, Hu H, Lin XH, et al. Euphorbia factor L_1 inhibited transport channel and energy metabolism in human colon adenocarcinoma cell line Caco-2. *Biomed Pharmacother*. 2023;169:115919. Available at: http://doi.org/10.1016/j.biopha.2023.115919
4. Zhan ZL, Liu X, Cheng ZH. Enhancing lathyrane structural diversity and MDR activity by combinatorial modification of lathyrane nucleus and ester side chain: A case study of Euphorbia Factor L_1 and Euphorbia Factor L_3. *Fitoterapia*. 2024;174:105854. Available at: http://doi.org/10.1016/j.fitote.2024.105854
5. Zhang JY, Lin MT, Yi T, et al. Apoptosis sensitization by Euphorbia factor L1 in ABCB1-mediated multidrug resistant K562/ADR cells. *Molecules*. 2013;18(10):12793–12808. Available at: http://doi.org/10.3390/molecules181012793
6. Neville D, Houghton R, Garrett S. Efficacy of plasma phospholipid removal during sample preparation and subsequent retention under typical UHPLC conditions. *Bioanalysis*. 2012;4(7):795–807. Available at: http://doi.org/10.4155/bio.12.38
7. Brooks MB, Stablein AP, Johnson L, Schultze AE. Preanalytic processing of rat plasma influences thrombin generation and fibrinolysis assays. *Vet Clin Pathol*. 2017;46(3):496–507. Available at: http://doi.org/10.1111/vcp.12534
8. Carmical J, Brown S. The impact of phospholipids and phospholipid removal on bioanalytical method performance. *Biomed Chromatogr*. 2016;30(5):710–720. Available at: http://doi.org/10.1002/bmc.3686
9. Kosjek T, Dolinšek T, Gramec D, et al. Determination of vinblastine in tumour tissue with liquid chromatography-high resolution mass spectrometry. *Talanta*. 2013;116:887–893. Available at: http://doi.org/10.1016/j.talanta.2013.08.009
10. Wu J. The Enhanced Permeability and Retention (EPR) Effect: The Significance of the Concept and Methods to Enhance Its Application. *J Pers Med*. 2021;11(8):771. Available at: http://doi.org/10.3390/jpm11080771
11. Shi Y, van der Meel R, Chen XY, Lammers T. The EPR effect and beyond: Strategies to improve tumor targeting and cancer nanomedicine treatment efficacy. *Theranostics*. 2020;10(17):7921–7924. Available at: http://doi.org/10.7150/thno.49577
12. Duan L, Yang L, Jin J, et al. Micro/nano-bubble-assisted ultrasound to enhance the EPR effect and potential theranostic

applications. *Theranostics*. 2020;10(2):462–483. Available at: http://doi.org/10.7150/thno.37593

13. Minardi S, Pandolfi L, Taraballi F, et al. PLGA-Mesoporous Silicon Microspheres for the in Vivo Controlled Temporospatial Delivery of Proteins. *ACS Appl Mater Interfaces*. 2015;7(30):16364–16373. Available at: http://doi.org/10.1021/acsami.5b03464
14. Wang HR ,Li TM ,He YP, et al. Quantitative correlation of ethyl cellulose-resveratrol microspheres' specific surface area with degradation, release, and stability performances over time. *Powder Technol*. 2025,452:120505. Available at: http://doi.org/10.1016/j.powtec.2024.120505
15. Manikandan S, Jose PA, Karuppaiah A, Rahman H. The effect of physical stability and modified gastrointestinal tract behaviour of resveratrol-loaded NLCs encapsulated alginate beads. *Naunyn Schmiedebergs Arch Pharmacol*. 2024;397(11):9007–9021. Available at: http://doi.org/10.1007/s00210-024-03223-3
16. Beltzer C, Hägele J, Kratz M, et al. Monitoring Degradation Process of PLGA/Cap Scaffolds Seeded WithMesenchymal Stem Cells in a Critical-Sized Defect in the Rabbit Femurusing Raman Spectroscopy. *J Bone Marrow Res*. 2013;1(4):1000133. Available at: http://doi.org/10.4172/2329-8820.1000133
17. Mohammad AK, Reineke JJ. Quantitative detection of PLGA nanoparticle degradation in tissues following intravenous administration. *Mol Pharm*. 2013;10(6):2183–2189. Available at: http://doi.org/10.1021/mp300559v
18. Hedberg EL, Kroese-Deutman HC, Shih CK, et al. In vivo degradation of porous poly (propylene fumarate)/poly (DL-lactic-co-glycolic acid) composite scaffolds. *Biomaterials*. 2005;26(22):4616–4623. Available at: http://doi.org/10.1016/j.biomaterials.2004.11.039
19. Cole AJ, David AE, Wang JX, Galbán CJ, Yang VC. Magnetic brain tumor targeting and biodistribution of long-circulating PEG-modified, cross-linked starch-coated iron oxide nanoparticles. *Biomaterials*. 2011;32(26):6291–6301. Available at: http://doi.org/10.1016/j.biomaterials.2011.05.024
20. Curcio A, Perez JE, Prévéral S, et al. The role of tumor model in magnetic targeting of magnetosomes and ultramagnetic liposomes. *Sci Rep*. 2023;13(1):2278. Available at: http://doi.org/10.1038/s41598-023-28914-4